Deliverable D4.3

Report on synthetic AFM systems

Project number	101070290
Project name	Nonlinear Magnons for Reservoir Computing in Reciprocal Space
Project acronym	NIMFEIA
Work package	WP4 – Materials and device fabrication
Type	Report
Dissemination level	Public
Lead beneficiary	Johannes Gutenberg University Mainz
Due date of delivery	Month 36

Authors: Gerhard Jakob, Mathias Kläui

Disclaimer:

The NIMFEIA project has received funding by the European Union's Research and Innovation Programme Horizon Europe under grant agreement No 101070290. However, views and opinions expressed in this document are those of the authors only and do not necessarily reflect those of the European Union. The European Union cannot be held responsible for them.

1. Development of materials and systems beyond state of the art: Synthetic Antiferromagnets.

1.1. Starting point and literature survey

Synthetic antiferromagnets (SAF) are composed of two ferromagnetic layers that are antiparallel exchange-coupled by a nonmagnetic thin interlayer through RKKY interaction. The latter is an oscillatory exchange coupling mediated by the conduction electrons of the interlayer material that oscillates and decays on the length scale of atomic distances depending on the Fermi vector of the material [1,2]. SAFs are long established in spintronics industry. The giant magnetoresistance (GMR) effect occurring when realigning the layers from antiparallel to parallel enabled a new generation of sensors and read heads for hard disk drives [3]. Due to the even bigger resistance changes in tunneling magnetoresistive devices (TMR) they have superseded GMR devices in many applications [4]. Most TMR devices also exploit SAFs, but only use them statically with the basic idea to reduce/tailor the magnetic stray field that the free layer experiences. The advantages that a SAF can offer with respect to improved dynamics and potential new functionalities have only recently come into focus. A short overview of the perspectives of SAF spintronics is presented by Duine at al. in [5]. Employing a compensated antiferromagnetic system minimizes the energy stored in the stray field and therefore enhances the dynamics. In addition, the nonferromagnetic system can have a Dzyaloshinskii-Moriya interaction with a neighboring ferromagnet and thus modify the type of domain walls and induce chirality in the system and the exchange coupling between the layers provides additional torques. Therefore e.g. a strongly enhanced domain wall velocity was observed by Yang et al. [6]. Coupled vortices of opposite polarity led to increased frequencies of the vortex dynamics and pushed the confined magnon spectra to higher frequencies [7]. While SAFs have been intensively investigated as discussed above, a key new aspect in particular for the control of confined spin structures is the control of the sign and the magnitude of the DMI. This is one of the significant factors for formation of skyrmions in SAFs. For that, it is indispensable that the sign of the DMI is controlled for both upper and lower ferromagnetic layers with interlayer exchange coupling which can be achieved by appropriately tuning the materials and interface properties that govern the DMI [8]. An obvious choice for the material is Pt as the bottom-heavy metal layer, because choosing it as a top heavy metal leads to decreasing interfacial DMI. W would also be one of the most appropriate candidates in terms of current induced skyrmion motion due to the giant spin-Hall angle previously identified [9]. As to interlayer exchange coupling materials, there were discussed different options; one is to use just one material (Ru, Ir, Rh) [10], another option is to use heterostructures such as Ru/Pt, Ir/Pt, Ir/Ru/Ir, or Pt/Ru/Ir. The former requires one to break spatial inversion symmetry using ferromagnets like Co/CoFeB, CoB/CoFeB, $[Co/Ni]_2$, or CoFeB with a gradient of composition along the thickness direction, otherwise the DMI might cancel between the top and bottom interfaces of the interlayer exchange coupling material [11]. For SAFs, the coupling between the layers as well as the anisotropy and DMI, which are all very sensitive to local structural variations, has shown to lead to significant pinning effects, which can make the spin structure poorly reproducible. For instance, it was previously shown that the Pt/Co system exhibits strong pinning, and thus, using polycrystalline Co as the ferromagnets is not an ideal choice and SAF skyrmions in Pt/Co systems have not been easily manipulated by currents [12].

1.2. Strategy and Methods

Here, we will focus on amorphous ferromagnets such as CoB, CoFeB, CoFeSiB, etc. where we have shown reduced pinning as there are no grain boundaries. Note that this simultaneously leads on average to a decrease of the magnetic anisotropy, DMI, and interlayer exchange coupling, which can depend on crystallization effects at interfaces. This makes it difficult to obtain systems with ultra-strong anisotropy and DMI as required, for instance, for extremely small skyrmions. Taking into account all of these effects, we developed a plan to deposit appropriate materials for the dynamics in SAF systems to be used in non-conventional computing. As a benchmark for the film quality, we investigate the formation of skyrmions and skyrmion diffusion, as the latter indicates low pinning in the magnetic system. We further investigate the coupling of such SAFs with skyrmions to their environment as well as skyrmion-skyrmion interactions, since the latter are nonlinear and therefore suitable for unconventional computing applications.

One interesting idea is to tune the strength of the interlayer exchange coupling during the application of the system by electric fields, as this is a highly promising and potentially effective approach for realizing energy-efficient applications. Recent interest has focused on the magneto-ionic effect in SAFs, driven by its potential to enable high-density data storage devices with ultra-low power consumption. However, the underlying mechanism responsible for the magneto-ionic effect on the interlayer exchange coupling remained elusive. Therefore, we created SAF stacks of composition Si(substrate)/SiO2(100nm)/Ta(5nm)/Pt(1.2nm)/Ir(0.4nm)/ $Co_{0.6}Fe_{0.2}B_{0.2}$(0.8nm)/Pt(1nm)/Ir(0.4nm)/$Co_{0.6}Fe_{0.2}B_{0.2}$(0.8-1.0nm)/HfO_2(3nm). On top of the HfO_2 layer, that serves as a source of oxygen for the metallic layers below, the ionic liquid 1-ethyl-3-methylimidazolium-bis(trifluormethylsulfonyl)imide [EMIM]þ[TFSI]_ was deposited and a glass substrate coated with indium tin oxide (ITO) was used as the top electrode. Different gating voltages were applied and the change of the magnetic response of the SAF system with perpendicular magnetic anisotropy was monitored by polar magneto-optical Kerr effect (MOKE), SQUID magnetometry and photoelectron spectroscopy. Figure 1 shows exemplary the high tunability of the magnetic response of the system to the electrical bias.

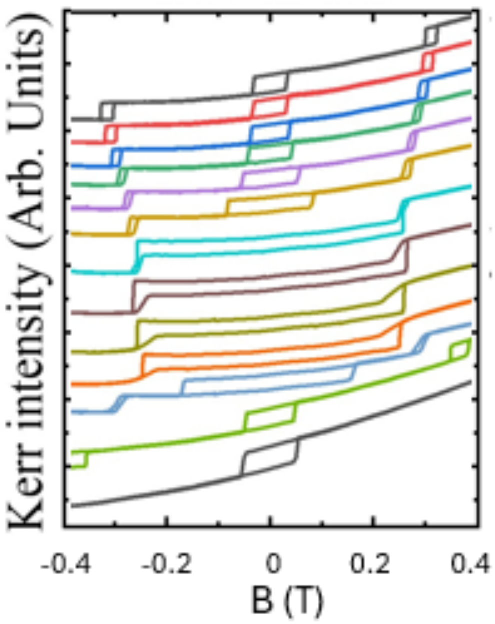

Figure 1: MOKE loops for SAF after different gating (order from top 0V, -0.8V, -1V, -1.2V, -1,4V, -1.6V, -1.8V, -2V, -2.2V,-2,4V, -2.6V, -2.8V, -3V, response vertically shifted). The ungated system (topmost) shows a switching at small fields, where the AFM coupling between the layers stays intact and both layers switch simultaneously with field, and a high field switching where the AFM coupling is broken by the external field H_{int}. Both fields undergo nonmonotonic variations with gating. The non-monotonic behavior of H_{int} as a function of the magnetic field was investigated for t_{CFB} of top FM equal to 0.9 nm. Hysteresis loops were recorded successively after each 30-s application of gating voltage. (Figure modified from [A]).

To understand the changes in magnetic properties, we investigated the modifications in chemical and electronic structure occurring due to the ionic liquid gating process using near-edge X-ray absorption fine structure (NEXAFS) spectroscopy and X-ray photoemission spectroscopy (XPS) measurements.

In our work, we found that the modulation of the interlayer exchange coupling is highly sensitive to the thickness of the ferromagnetic layer. We have identified that the changes in the interlayer exchange coupling induced by the gate voltage can be associated with the magneto-ionic effects on the top ferromagnetic layer of the SAF. The direct contact between the high ion mobility oxide and the top ferromagnetic layer plays a crucial role in facilitating these effects, largely modifying the anisotropy of the layers. A detailed scientific discussion of the results was published in Applied Physics Letters [A].

One big advantage of SAF devices is their negligible stray field. This leads to higher possible device densities and potentially ultrafast dynamics prompting a shift towards antiferromagnetic topological spin textures as information carriers. In addition to skyrmions, which are topological spin structures in perpendicular magnetized systems we realized such chiral in-plane topological antiferromagnetic spin textures namely merons, antimerons, and bimerons in SAFs by concurrently engineering the effective perpendicular magnetic anisotropy, the interlayer exchange coupling, and the magnetic compensation ratio. An ideal system to explore and manipulate both structural and dynamical properties of topological spin textures are SAF platforms as those we report in [B]. They consist of a multilayered heterostructure made of ferromagnetic thin films separated by nonmagnetic metallic spacers and antiferromagnetically coupled via the interlayer exchange interaction. We tailored the amount of compensation such that they exhibited an arbitrarily small magnetic moment and, therefore, combine the most interesting features of both ferromagnetic and antiferromagnetic scenarios: minimal stray fields, the ability to stabilize homochiral spin textures, and the potential for ultrafast spin dynamics; all in a device compatible easy-to-fabricate polycrystalline multilayer setting. A precondition to assess the topological nature of such spin textures is to be able to measure their chirality. In this regard, SAFs offer the advantage to employ the advanced surface- or element-sensitive imaging methods available for ferromagnets. Spontaneously formed stable homochiral spin textures on a global scale have hitherto not been reported before our work. The ferromagnetic films consist of the bilayer $Fe_{0.6}Co_{0.2}B_{0.2}$(FCB)/$Co_{0.6}Fe_{0.2}B_{0.2}$(CFB) and are sandwiched between the nonmagnetic spacers Pt and Ir. This breaks the mirror symmetry of the heterostructure, thus providing a finite DMI. Experimentally we employed scanning electron microscopy with polarization analysis (SEMPA) to image the in-plane component of the magnetic spin texture. This is a surface-sensitive technique, that we can use in house at our partner JGU. It uses the spin-polarized secondary electrons emitted from a magnetic material and gives a two-dimensional (2D) vector map of the in-plane magnetization as shown in Figure 2. The sensitivity of SEMPA is limited to 1−2 nm depth from the surface, which enables us to image the topological spin textures present only in the topmost magnetic layer. This unique feature of SEMPA is especially effective on SAFs and allows us to investigate the formation of topological spin textures even in a fully compensated composition.

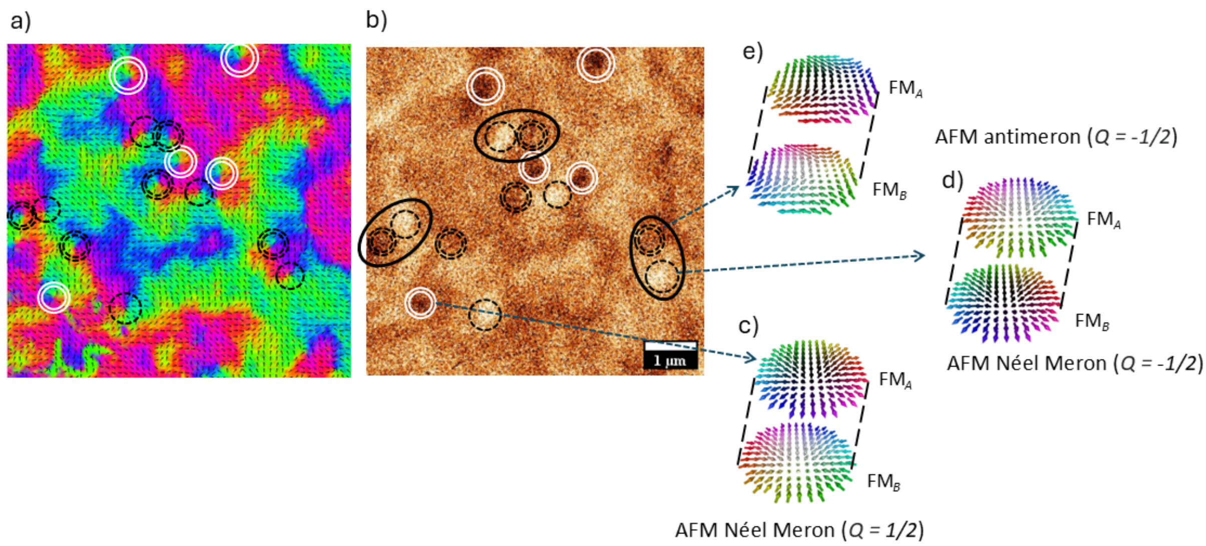

Figure 2: (a) SEMPA image showing the in-plane (IP) spin components of the topmost ferromagnetic FM_A layer, or, equivalently, the IP component of the Néel order of the meron textures. (b) Magnetic force microscopy (MFM) image showing the out-of-plane (OOP) spin component of the FM_A layers, that is the OOP component of the Néel order of the meron structures in the same area. Dark brown and white MFM contrasts indicate the upward and the downward direction, respectively. Black dotted circles represent merons of helicity $\gamma = \pi$, whereas double black dotted circles indicate antimerons, both with Q = -½. White circles represent merons having an arbitrary helicity with Q = ½ and white double circles denote merons of helicity $\gamma = 0$ and Q = ½. Two adjacent black circles (single and double) are identified as bimerons with net topological charge $Q = -1$ and are additionally highlighted by ellipses. (c) An AFM Néel meron having $\gamma = 0$ and Q = ½, (d) an AFM Néel meron having $\gamma = \pi$ and Q = -½. (e) an AFM antimeron having Q = -½. (Figure modified from [B]).

Our experiments show the existence of room-temperature stable bimerons in compensated SAFs at zero external magnetic fields. We have developed an analytical model and performed micromagnetic simulations using experimentally extracted parameters to explain the stability of the chiral topological structures in zero magnetic field. Based on the input parameters, we can construct phase diagrams of the observed topological structures in the SAF system. We could demonstrate multimodal vector imaging of the three-dimensional Néel order parameter, revealing the topology of those spin textures and a globally well-defined chirality, which is a crucial requirement for controlling current-induced dynamics. Our analysis revealed that the interplay between interlayer exchange and interlayer magnetic dipolar interactions plays a key role to significantly reduce the critical strength of the DMI required to stabilize topological spin textures, such as antiferromagnetic merons, in SAFs, making them a promising platform for next generation spintronics applications. An in-depth discussion of the respective results was published in Nature Communications in reference [B].

Scattering analysis offers a fundamental route to revealing particle interactions with direct implications for device technologies relying on ensembles of particles such as magnetic skyrmions. To investigate skyrmion-skyrmion interactions as well as the transient response to the spin torque of the SAF skyrmion lattice, we prepared and optimized a low-pinning SAF stack comprising thin multilayers with two alternating ferromagnetic sublattices (A and B). To probe the particle interactions, the magnetic system was tuned to obtain full magnetization compensation, as evidenced by the hysteresis curves measured using a SQUID magnetometer. The strategic incorporation of Fe-rich and Co-rich ferromagnetic layers into the two ferromagnetic sublattices enabled independent probing of each sublattice via X-ray imaging using the corresponding absorption edges at a synchrotron and thus provided a direct method to visualize the antiferromagnetic skyrmion lattice. The uniqueness of our experimental setup opened the door to sublattice-resolved studies of pinning potentials as well as transient response, a key determinant of spin-texture dynamics in any magnetic systems with multiple sublattices. Scanning transmission X-ray microscopy (STXM) performed at the Fe L3 and Co L3 absorption edges revealed an inverted skyrmion contrast between sublattices A and B. This inversion reflects the antiparallel out-of-plane magnetization in adjacent layers, confirming robust antiferromagnetic interlayer exchange coupling across the multilayer stack. Within this framework, skyrmions in sublattice A exhibit a topological charge of $Q_A = +1$, whereas those in sublattice B carry $Q_B = -1$. Together, they constitute a SAF skyrmion lattice.

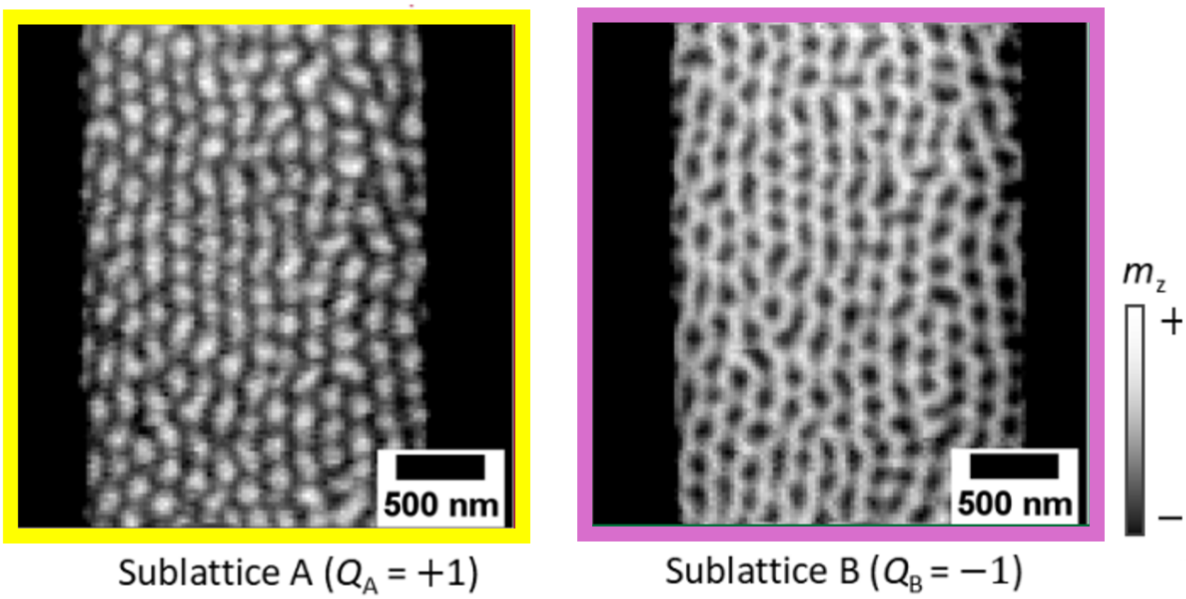

Figure 3: Static imaging of the antiferromagnetic skyrmion lattice taken at the identical magnetic external field strength of -0.25T. The SAF multilayer was stack composed of Fe-rich (sublattice A, yellow) and Co-rich (sublattice B, pink) ferromagnetic layers, antiferromagnetically coupled via Ir spacers. Sublattice-selective X-ray imaging of the antiferromagnetic skyrmion lattice at the Fe (left) and Co (right) L_3 absorption edges. The inverted magnetic contrast between sublattices confirms robust antiferromagnetic coupling of the skyrmion lattice throughout the multilayer. (Figure modified from [C]).

We have driven the skyrmion lattice using short current pulses and imaged the response in real time by synchronizing with the X-ray pulses from the synchrotron. In the low-current regime ($J = 2.8\times10^{11}$ A/m^2), where the strength of the current-induced spin-orbit torques is comparable to the local pinning potential, the motion is governed by a spatially inhomogeneous energy landscape. In this case, variations in pinning strength give rise to an incoherent dynamical regime in which different parts of the lattice respond differently to the same uniform drive. Despite the application of a uniform current, the lattice response is spatially heterogeneous: some skyrmions remain pinned. Pinned skyrmions act as rigid obstacles within the lattice, inducing constraints that can be described in a mechanics approach and lead to anisotropic strain in neighboring skyrmions. As adjacent skyrmions are pushed by under the applied current, these constraints result in boundary elongation or compression. The complex behavior of the individual skyrmion motion allowed us to extract the skyrmion interaction potential directly from the nanosecond relaxation dynamics of skyrmions, which lie at the lateral boundary between mobile and pinned regions. In this geometry, the pinned skyrmions act as fixed scattering centers, providing boundary conditions for quantifying the skyrmion–skyrmion interaction potential.

We tracked the experimentally measured recoil trajectories of the skyrmions following the termination of the nanosecond current pulse and employed an inverse estimation based on the Thiele equation. For high current regimes, all skyrmions could be unpinned, and we observed a coherent flow, where the lattice translates uniformly. Quantification of the reproducible post-pulse relaxation trajectories via an inverse analysis method based on the Thiele equation yields the nanoscale skyrmion–skyrmion scattering potential, which decays exponentially with a range of 30 nm, in full agreement with micromagnetic simulations. At higher current densities, the lattice exhibits coherent motion free from detectable Hall and inertial effects or dynamical deformation, enabling robust GHz operation. These findings establish a quantitative framework for SAF skyrmion interactions and demonstrate deterministic control of their collective dynamics over billions of cycles even in the incoherent flow regime, thereby paving the way for multi-skyrmion spintronic devices. Details of these results are currently submitted for publication in a peer reviewed journal and the manuscript is available under reference [C].

The work described above was done on SAFs that showed essentially two-dimensional magnetic structures despite their multilayered structure with the different ferromagnetic layers showing opposite magnetic behavior. Those 2D spin structures exhibit fully reciprocal dynamics as there are no symmetry-breaking mechanisms available due to their limited complexity. On the other hand, 3D topological spin textures beyond 2D magnetic skyrmions, such as skyrmion tubes offer additional perspectives for devices. It has been shown that the more complex dynamics of such 3D spin configurations enable novel functionality such as triggering extremely non-linear electromagnetic responses, which leads to advanced skyrmionic applications, including skyrmion-based logic with diodes and neuromorphic computing, where one of the indispensable crucial components is the non-reciprocal dynamics of the topological objects.

In thin-film multilayer systems or SAFS with an interfacial DMI, a hybrid chiral skyrmion tube is an archetypal example of a 3D topological spin texture. Hybrid chiral skyrmion tubes can emerge due to the energy competition between long-range dipole interaction and interfacial DMI. Their structure uniquely exhibits twisting of the helicity across the thickness direction, which can result in intrinsically distinct dynamics compared to that of conventional skyrmion tubes with homogeneous chirality. However, such possibly unique dynamics of the hybrid chiral skyrmion tubes have not been demonstrated, so it is unclear if these 3D topological spin structures could be apt for active elements in spintronic applications. To realize such skyrmions tubes we modified the Fe/Co ratio in SAF multilayers from Co rich at the bottom layers to Fe rich at the top layers, which inverts the direction of the DMI along the direction perpendicular to the layer. The stack structures consisted of Ta(5.00)/[Pt(1.00)/Ir(0.40)/FM_{B1}/Pt(1.00)/Ir(0.40)/$FM_{T1}]_{\times 15}$/Pt(1.00) (numbers in nm) (ST1, hereafter), and Ta(5.00)/[Pt(1.00)/Ir(0.40)/FM_{B2}/Pt(1.00)/ Ir(0.40)/$FM_{T2}]_{\times 25}$/Pt(1.00) (ST2, hereafter), respectively, deposited on 100 nm-thick silicon nitride membrane substrates. The FM_B and FM_T layers are addressed as a bottom (Co-rich) ferromagnetic and top (Fe-rich) ferromagnetic layer, respectively, and they are anti-ferromagnetically coupled via the Pt/Ir interlayers. For imaging, we used an element-specific detection technique: scanning transmission X-ray microscopy (STXM) with magnetic circular dichroism as the contrast mechanism. This demonstrated the interlayer AFM coupling that led to fully coupled skyrmions in the layers. Current pulses synchronized with the X-ray pulses enabled imaging of the dynamic behavior. From the statistical evaluation of the movement of the skyrmions tubes one can calculate the average skyrmions velocity. For a quantitative evaluation of the skyrmion Hall effect, we employed the same protocol as for the skyrmion velocity, where the averaged skyrmion Hall angle, θ_{ave}, is extracted from the peak of the Gaussian fitting. We find that the values of θ_{ave} are reciprocal for both current pulse polarities at υ_{ave} = 10 m/s, which corresponds to the creep/depinning regime. Surprisingly, we find an intriguing behavior for the higher velocity in the flow regime of $\upsilon_{ave} = 25$ m/s, where the degeneracy of two Gaussian peaks regarding the current polarity is distinctly lifted, indicating the presence of a non-reciprocal skyrmion Hall effect in the flow regime.

Figure 4: Examples of the tracked current induced motion of SAF skyrmions tubes. Current flow is in perpendicular direction and from the transverse deflection the skyrmion Hall angle is calculated. The figure is modified from Fig. 2 in [D].

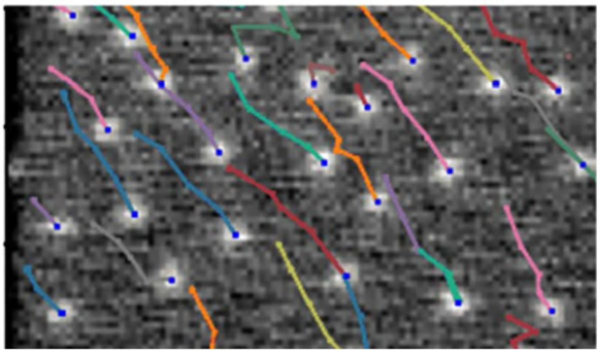

The spin structure of the skyrmion tube obtained from relaxation at zero field using micromagnetic simulations provides further insights into the effect of magnetic compensation on the equilibrium structure. These simulations reveal that the skyrmion helicity varies across different layers due to net stray fields arising from the net magnetization in the multilayer system and varies with the applied current. Our theoretical modeling qualitatively corroborates that the non-reciprocity stems from the dynamic oscillation of skyrmion helicity during its current-induced motion. The findings highlight the critical role of the internal degrees of freedom of these complex skyrmion tubes for their current-induced dynamics. An in-depth discussion of the respective results is published in Nature Communications in reference [D].

For the sake of completeness, we shortly report on other aspects of skyrmion dynamics and interactions, which we studied in relation to NIMFEIA. In Ref. [E], we investigated the effects of chiral polypeptides on skyrmion stability and dynamics and published the results in Nano Letters. In Ref. [F], we studied the change of the dynamics in coupled magnetic layers, where one undergoes a magnetic compensation and has zero moment like a properly tuned SAF, and published the findings in Phys. Rev. B. The role of dipolar interactions in skyrmion lattices was studied in Ref. [G]. In Ref. [H], we focused on the ultrafast dynamics of chiral spin structures in antiferromagnets and published the findings in Phys. Rev. B.

1.3. Summary and conclusions

In conclusion, we made a broad investigation of the potential of SAFs for applications relevant to NIMFEIA based on complex material stacks that were tailored for the specific scientific questions to be solved within Task 4.3. More detailed results than mentioned in this report can be found in the scientific papers that are published with NIMFEIA acknowledgements in [A]-[H]. These papers discuss partly also topics that are outside the scope of NIMFEIA.

2. Publications

[A] **Magneto-ionic modulation of the interlayer exchange interaction in synthetic antiferromagnets,**
Maria-Andromachi Syskaki, Takaaki Dohi, Sergei Olegovich Filnov, Sergey Alexeyevich Kasatikov, Beatrice Bednarz, Alevtina Smekhova, Florian Kronast, Mona Bhukta, Rohit Pachat, Johannes Wilhelmus van der Jagt, Shimpei Ono, Dafiné Ravelosona, Jürgen Langer, Mathias Kläui, Liza Herrera Diez, and Gerhard Jakob,
Appl. Phys. Lett. **124**, 082408 (2024), doi: 10.1063/5.0198750

[B] **Homochiral antiferromagnetic merons, antimerons and bimerons realized in synthetic antiferromagnets,**
Mona Bhukta, Takaaki Dohi, Venkata Krishna Bharadwaj, Ricardo Zarzuela, Maria-Andromachi Syskaki, Michael Foerster, Miguel Angel Niño, Jairo Sinova, Robert Frömter, and Mathias Kläui,
Nature Communications **15**, 1641 (2024), doi: 10.1038/s41467-024-45375-z .

[C] **Antiferromagnetic Skyrmion Scattering Revealed by Direct Time-Resolved Imaging of Collective Dynamics**
Mona Bhukta, Takaaki Dohi, Kilian Leutner, Maria-Andromachi Syskaki, Fabian Kammerbauer, Duc Minh Tran, Sebastian Wintz, Markus Weigand, Robert Frömter, and Mathias Kläui,
arXiv2508.17967 (2025) https://arxiv.org/pdf/2508.17967

[D] **Observation of a non-reciprocal skyrmion Hall effect of hybrid chiral skyrmion tubes in synthetic antiferromagnetic multilayers**
Takaaki Dohi, Mona Bhukta, Fabian Kammerbauer, Venkata Krishna Bharadwaj, Ricardo Zarzuela, Aakanksha Sud, Maria-Andromachi Syskaki, Duc Minh Tran, Thibaud Denneulin, Sebastian Wintz, Markus Weigand, Simone Finizio, Jörg Raabe, Robert Frömter, Rafal E. Dunin-Borkowski, Jairo Sinova, and Mathias Kläui,
Nat. Commun (accepted 27th Aug. 2025) https://doi.org/10.1038/s41467-025-63759-7

[E] **Effects of Chiral Polypeptides on Skyrmion Stability and Dynamics**,
Yael Kapon, Fabian Kammerbauer, Theo Balland, Shira Yochelis, Mathias Kläui, and Yossi Paltiel,
Nano Lett. 25, 306−312 (2025) https://pubs.acs.org/doi/10.1021/acs.nanolett.4c05035

[F] **Temperature dependent study of the spin dynamics of coupled $Y_3Fe_5O_{12}$/$Gd_3Fe_5O_{12}$/Pt trilayers**,
Felix Fuhrmann, Sven Becker, Akashdeep Akashdeep, Gerhard Jakob, Qianqian Lan, Nan Wang, Rafal E. Dunin-Borkowski, Romain Lebrun, Mathias Weiler, and Mathias Kläui,
Phys. Rev. B 112, 064432 (2025), https://doi.org/10.1103/7d4q-j8cl

[G] **The role of magnetic dipolar interactions in skyrmion lattices,**
E. M. Jefremovas, K. Leutner, M.G. Fischer, J. Marqués-Marchán, T.B. Winkler, A. Asenjo, J. Sinova, R. Frömter, and M. Kläui,
Newton, ***1***(2), 100036-100036, (2025) https://doi.org/10.1016/j.newton.2025.100036

[H] **Ultrafast dynamics of chiral spin structures in synthetic antiferromagnets**,
Z. Guo, R. Gruber, D. Ksenzov, C. Leveille, M. Pancaldi, E. Pedersoli, C. Spezzani, G. De Ninno, F. Capotondi, C. Gutt, M. Klaeui, V. Cros, N. Reyren, and N. Jaouen,
Phys. Rev. B **112**, L020408 (2025) https://doi.org/10.1103/1f11-n7dc

3. References

[1] Grünberg, P., R. Schreiber, Y. Pang, M.B. Brodsky, and H. *Sowers, Layered magnetic structures: Evidence for antiferromagnetic coupling of Fe layers across Cr interlayers*, Phys. Rev. Lett. **57**, 2442–2445 (1986).

[2] Parkin, S., N. More, and K. Roche, *Oscillations in exchange coupling and magnetoresistance in metallic superlattice structures: Co/Ru, Co/Cr, and Fe/Cr*, Phys. Rev. Lett. **64**, 2304 (1990).

[3] Thompson, Sarah M., *The discovery, development and future of GMR: The Nobel Prize 2007*, J. Phys. D: Appl. Phys. **41** 093001 (2008).

[4] Parkin, S., Xin Jiang, C. Kaiser, A. Panchula, K. Roche, and M. Samant, *Magnetically engineered spintronic sensors and memory*, Proceedings of IEEE **91**, 661 (2003)

[5] Duine, R., K.J. Lee, S.S. Parkin, and M.D. Stiles, *Synthetic antiferromagnetic spintronics*, Nat. Phys. **14**, 217–219 (2018).

[6] Yang, S.-H., R. Kwang-Su, and S Parkin, *Domain-wall velocities of up to 750 m s^{-1} driven by exchange-coupling torque in synthetic antiferromagnets,* Nature Nanotechn. **10**, 221–226 (2015).

[7] Cherepov, S.S., B. C. Koop, A. Yu. Galkin, R. S. Khymyn, B. A. Ivanov, D. C. Worledge, and V. Korenivski, *Core-Core Dynamics in Spin Vortex Pairs*, Phys. Rev. Lett. **109**, 139902 (2012).

[8] Guan, Y., T. Koyama, and D. Chiba, *Current-induced magnetic domain wall motion in Pt/Co/Pd and Pd/Co/Pt structures with opposite sign of Dzyaloshinskii-Moriya interaction*, AIP Advances **7**, 085123 (2017).

[9] Pai, C.-F., L. Liu, Y. Li, H. W. Tseng, D. C. Ralph, and R. A. Buhrman, *Spin transfer torque devices utilizing the giant spin Hall effect of tungsten*, Appl. Phys. Lett. **101**, 122404 (2012).

[10] Parkin, S., Systematic variation of the strength and oscillation period of indirect magnetic exchange coupling through the 3d, 4d, and 5d transition metals, Phys. Rev. Lett. **67**, 3598 (1991)

[11] Jamali, M., K. Narayanapillai, X. Qiu, L. Ming Loong, A. Manchon, and H. Yang, *Spin-Orbit Torques in Co/Pd Multilayer Nanowires*, Phys. Rev. Lett. **111**, 246602 (2013).

[12] Chen, R., Y. Gao, X. Zhang, R. Zhang, S. Yin, X. Chen, X. Zhou. Y. Zhou, J. Xia, Y. Zhou, S. Wang, F. Pan, Y. Zhang, and C. Song, *Realization of Isolated and High-Density Skyrmions at Room Temperature in Uncompensated Synthetic Antiferromagnet*, Nano Lett, **20**, 3299 (2020).